Conversion and amplification of photomultiplier anode current in multiple-frequency phase fluorometry

K. Hädener, S. Bergamasco, and G. Calzaferri

Institute for Inorganic and Physical Chemistry, University of Berne, Freiestrasse 3, CH-3000 Berne 9, Switzerland

(Received 22 January 1988; accepted for publication 18 May 1988)

We have designed and built a low-cost current–voltage converter with a bandwidth larger than 200 MHz and a fixed ac insertion gain of 20 dB for use in multiple-frequency phase fluorometry (MFPF). We describe its application with the Hamamatsu R928 photomultiplier (PMT) and discuss problems of radio-frequency (rf) interference, signal-to-noise ratio (S/N), PMT nonlinearity, and overall frequency bandwidth. The separation of ac and dc signal paths introduces the possibility of direct determination of relative modulation in two simultaneous measurements. We demonstrate that systematic errors such as PMT nonlinearity can be completely eliminated in MFPF by an appropriate experimental procedure and report an accuracy of our dual-beam instrument of 5 ps.

INTRODUCTION

Over the past decade multiple-frequency phase fluorometry (MFPF) has advanced to a well-established technique for the investigation of luminescence characteristics.[1–10] The availability and use of lasers as excitation sources and stable electro-optic modulators covering a broad, continuous frequency spectrum have promoted the development of research instruments and led to the commercialization of the method as well.[11]

Introducing cross correlation of the fluorescence signal with a second high-frequency source has considerably improved the sensitivity of the frequency-domain technique, with the disadvantage of relying on several detectors in most instruments.[7,9,11] Small side-on photomultipliers (PMT) such as the Hamamatsu 1P28, R928, and R446 have found widespread use as light detectors in these fluorometers; only recently have they been partly replaced by microchannel plates such as the fast Hamamatsu R1564U for the special case of modulation by the harmonic content of a pulse train from a cavity dumped dye laser[12,13] where the mean detector current is small.

Considerable effort has been spent on optimizing the rise-time characteristic of the inexpensive side-on-type PMT's by modification of the high-voltage divider network.[7,9,14–16] As claimed by Köchel *et al.*,[17] however, for the case of the R928 circular cage PMT, the optimum mode of operation with respect to the noise factor is the one with standard, constant interstage voltage distribution.

According to our experience many of the dominating PMT-related problems in phase fluorometry do not originate in the dynode circuitry, but in inappropriate anode current pathways.

I. REQUIREMENTS

Considering the frequency band applied in the MFPF technique, coaxial cables with a characteristic impedance of 50 Ω and external amplifiers/analyzers of the same input impedance are generally used. Hence, termination of the detector output into a pure resistance of 50 Ω is required to minimize waveform distortions and ringing phenomena caused by power reflection.

The resulting detector cutoff frequency found from the corresponding $R \times C$ product is nonlimiting as long as the total capacitance of the PMT anode relative to all other dynodes, including stray capacitances caused by wiring, is kept at a minimum. Broadband, low-noise amplification becomes necessary in those cases, where the voltage resulting from a PMT anode current across 50 Ω is too small for the phase fluorometer detection setup; at this stage dc coupling has to be preserved in order to allow measurements of the relative modulation of the detector signal.

II. DESCRIPTION OF THE DEVICE

Based on considerations of radio-frequency (rf) interference the TE-146-TSRF (Products for Research) thermoelectric heat-exchanged cooled housing was chosen because of its thorough shielding. Compared to a standard potted tube socket, the extended socket assembly (Products for Research) employed provided additional volume (39×81-mm diam) for incorporating the converter/amplifier circuit.[18] The socket wiring consisted of ten resistors of 330 kΩ each with three capacitors of 10 nF/1 kV parallel to the last three resistors in the chain and of a simple rf decoupling shield contact element. The insulating window of the housing was exchanged for a fiber-optic feedthrough of multilayered PVC. The outer surface of the feedthrough was covered with a sheet of blank copper.

The basic idea of our circuit is to separate ac and dc paths in order to avoid the problem of dc-coupled amplification of a high-frequency signal. Once the two components were separated, standard low-cost elements could be used and thus the schematic diagram shown in Fig. 1 looks very simple.

With the OP27 a standard operational amplifier is used for current–voltage transformation in the dc path. With a value of 30 kΩ for the metal film feedback resistor a dc out-

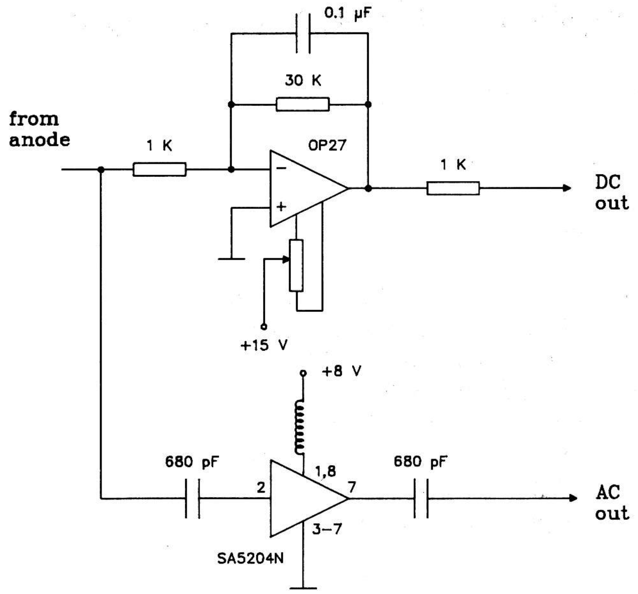

FIG. 1. Circuit diagram of the current–voltage converter as used with the R928 PMT.

put voltage of 3 V results for the maximum allowed anode current of 100 μA and the offset of the OP27 can be compensated by a small potentiometer.

With a fixed insertion gain of 20 dB the low-cost SA5204N (Philips Linear Products) performs high-frequency amplification; its gain is flat to 0.5 dB from dc to 200 MHz, with a -3-dB bandwidth greater than 350 MHz. Since the part is internally compensated and matched to 50 and 75 Ω, no external components are needed other than ac coupling capacitors. Stray capacitance problems are minimized by the amplifier's layout as a small, monolithic integrated circuit die.

The circuit was implemented on a 75-mm-diam epoxy print by a ground plane technique. Two SMA bulkhead feed-through jack receptacles were mounted in the socket chassis for the ac and dc signals; the dc power lines were rf decoupled inside the socket.

Consequent use of high-quality semirigid-type coaxial cables has proved to be fundamental to achieving satisfactory signal-to-noise (S/N) ratios.

III. PERFORMANCE TESTING

A. Linearity with anode current

An important characteristic of a PMT/amplifier combination is output voltage linearity with incident light intensity. Any method for luminescence lifetime determination relying on two or more distinct measurements of different light intensities assumes detector linearity.

Our detector setup, with a two-arm bundle of fused silica fibers that end, statistically mixed, about 20 mm from a well-defined spot on the PMT's cathode, allowed a linearity check as a simple experiment. Successively increasing equal light intensities [530.9-nm Kr^+, attenuated by Glan–Taylor prisms, scattered by 0.3% LUDOX HS (DuPont) solutions] were coupled into the sample arm; then the reference arm; and finally, into both arms of the fiber bundle simultaneously: The corresponding dc detector output was recorded.

Provided that the R928 PMT's with the current–voltage converter were operating linearly, the sum of the particular sample and reference signals $V(S)$ and $V(R)$ should have equaled the sum signal $V(S+R)$ at any level of incident light power. Figure 2, which shows a plot of the ratio $V(S+R)/[V(S)+V(R)]$ vs $V(S)+V(R)$, should then have consisted of the dashed line parallel to the abscissa. The experiment revealed a considerable degree of nonlinearity, reaching a deviation of nearly 10% at $\frac{2}{3}$ of the maximum anode current. This over-response may be fully attributed to the R928 PMT–dynode string combination; it is caused by an increase in dynode voltage resulting from the redistribu-

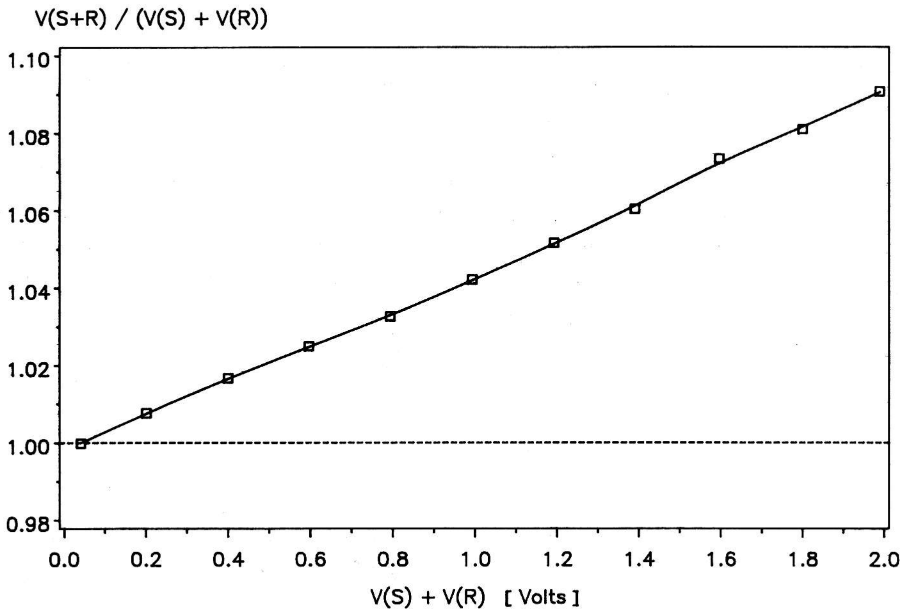

FIG. 2. Nonlinear response of the R928 PMT for dc signals. $HV = -1000$ V, 25 °C.

tion of the voltage loss between the last dynode and the anode[19] and can be diminished by increasing the voltage-divider current compared to the anode output current. In addition, direct anode current measurements with the RCA 31024 PMT in an analogous experiment[8] have yielded even larger deviations from linearity, showing a beginning saturation near the value of the current flowing through the voltage divider due to the extension of voltage losses to the last few stages. The magnitude of deviations even at low anode current levels apparent from Fig. 2 imperatively calls for a nonlinearity correction as developed for our setup[8,10] or for a proper measurement procedure in order to avoid systematic errors.

B. Frequency bandwidth

To characterize the frequency response of the detection system, ac and dc components of the signal produced by Rayleigh scattered light were monitored as a function of modulation frequency. The 530.9-nm output of a Kr^+ laser (Spectra Physics model 171) was sinusoidally modulated by an acousto-optic modulator (Intra Action AOM 403) at 1700 Hz. The zeroth-order beam was then modulated at variable frequency by an electro-optic modulator (Conoptics model 380) driven by a tracking generator (Tektronix TR501) and a rf power amplifier (ENI model 550L). Ordinary (O-) and extraordinary (E-) output of the second modulator was directed into two translation stages and finally, onto two 10-mm fused silica cells containing 0.3% LUDOX HS solutions. The scattered light was coupled into the two arms of the optical fiber bundle ending on the PMT. The ac component of the detector signal (first sideband) was monitored on a spectrum analyzer (Tektronix model 7L13) with 30-Hz resolution, whereas the dc voltage was measured with a digital multimeter (Schlumberger model 7060). Both signals were individually recorded for the O- and E-beams as a function of modulation frequency in the range of 15–170 MHz; the results are shown in Fig. 3.

A first inspection of the plot in Fig. 3 suggests separate discussion of the frequency response for the two bands up to and above 90 MHz. Below this limit the characteristics are essentially flat, with a small decrease in relative modulation due to the electro-optic modulator, but identical levels for both beams. Above 90 MHz a considerable loss in signal in the E- compared to the O-beam is noticed. The concerted vanishing of both ac and dc components is a consequence of increasing E-beam divergence due to limited modulator performance. The same phenomenon is observed, to a smaller extent, for the O-beam. The unproportional decrease of the ac signal part in both cases is exactly accounted for by the finite rise time of 2.2 ns of the R928 PMT[19]; the pronounced maximum at 145 MHz can also be attributed to the electro-optic modulator's peculiarities. Thus far we have not been able to give a definite explanation for the observed asymptotic disappearance of both dc signal components approaching 200 MHz. However, all the reported details that describe a degradation of frequency response are independent of the current–voltage converter employed, as this experiment has been cross checked against direct anode current measurements on the same PMT tube.

C. Overall accuracy

With regard to the reported relatively large deviation from linearity of the detection system, the question of overall accuracy of the MFPF fluorometer employed arises.

The standard procedure for testing this condition in our dual-beam phase fluorometer makes use of the motorized translation stage installed that allows variation in the optical path of the O- beam by as much as 300 cm with a resolution

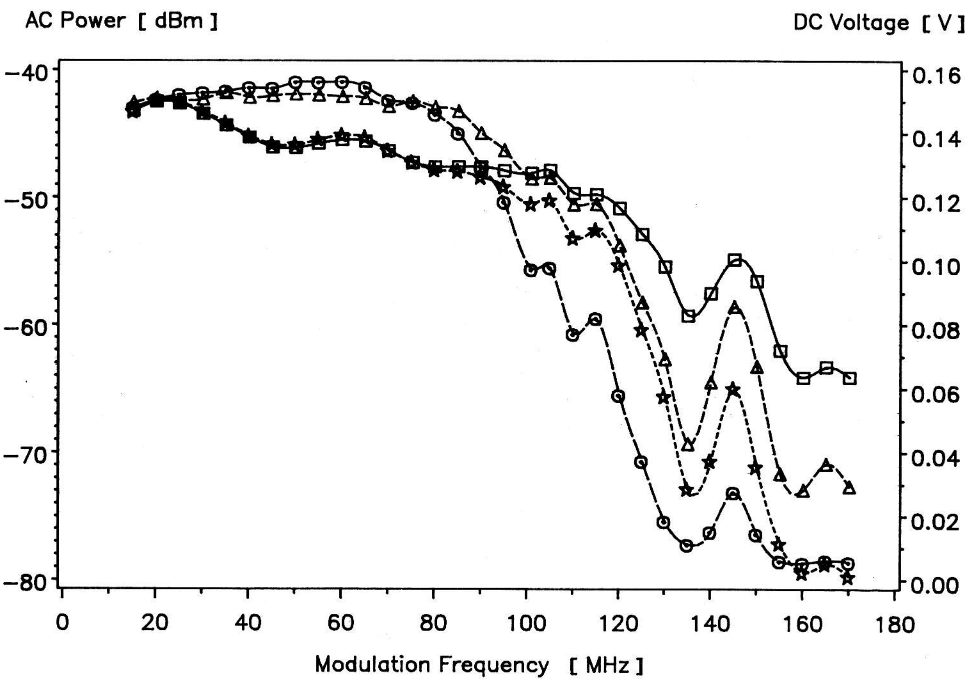

FIG. 3. ac and dc detector signals as a function of modulation frequency. $HV = -1000$ V, 25 °C. □, ac O-beam; ☆, ac E-beam; △, dc O-beam; ⊙, dc E-beam.

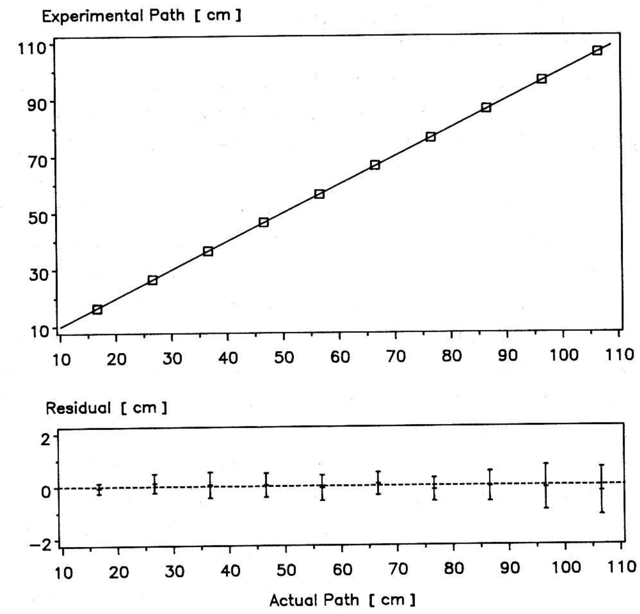

FIG. 4. Overall accuracy check of the double-beam MFPF instrument with current–voltage converter and R928 PMT. $HV = -1000$ V, 25 °C, $f = 50$ MHz; mean dc current $\bar{i}_{dc} = 6\ \mu$A.

of 100 μm. Comparison of the optical delay introduced by the delay line with the measured phase difference $\Delta\Phi$, using

$$L = c\Delta\Phi/\omega, \qquad (1)$$

where L is the measured path difference, ω is the circular frequency, and c is the velocity of light, not only yields the experimental precision, but also yields the absolute accuracy of our setup. The result of such an experiment is shown in Fig. 4. The distribution of the residuals indicates a mean deviation of a single phase difference determination corresponding to less than 5 ps, whereas the standard deviation given in Fig. 4 as confidence intervals computed from experimental entities by error propagation is slightly overestimated. We would like to stress that prior to nonlinearity correction as described in Refs. 8 and 10 the residuals of Fig. 4 deviate systematically from zero and for the most part are not even compatible at the overestimated 95% confidence level.

IV. DISCUSSION

Application of the current–voltage converter designed for use with the R928 PMT, supported by the additional means of shielding described above, has led to an improvement in the S/N ratio of up to 30 dB over direct anode current measurements. Definite and proper output impedance along with a frequency bandwidth considerably larger than that of the limiting components in our setup can be regarded as the dominating converter circuit's contribution to this enhancement. The device has met the demands in phase fluorometric determination of the decay kinetics of 10^{-6} molar rhodamine 3B and pyronine B solutions in dioxane–water and glycerol–water mixtures. Measurements were carried out at emission wavelengths between 550 and 685 nm with 4-nm resolution and with modulation frequencies between 30 and 138 MHz; detailed results of these experiments are given elsewhere.[20]

Using benzene as a Raman scatterer (3047 and 3062 cm^{-1}) and the 406.7-nm Kr^+ laser lines (50 mW) for excitation, a value for the R928 PMT's color effect of less than 0.19 ps/nm was found, in very good agreement with Ref. 15.

ACKNOWLEDGMENTS

This work was supported by Grant No. 2.025-0.86 from the Swiss National Science Foundation. We would like to thank Dr. Thomas Hugentobler for his contributions to the experimental part. KH offers his special thanks to Kurt von Escher and W. Amacher for their assistance in realizing the current–voltage converter circuit.

[1] H. P. Haar and M. Hauser, Rev. Sci. Instrum. **49**, 632 (1978).
[2] H. Gugger and G. Calzaferri, J. Photochem. **13**, 21 (1980).
[3] H. Gugger and G. Calzaferri, J. Photochem. **13**, 295 (1980).
[4] H. Gugger and G. Calzaferri, J. Photochem. **16**, 31 (1981).
[5] J. Baumann and G. Calzaferri, J. Photochem. **22**, 297 (1983).
[6] J. Baumann and G. Calzaferri, J. Photochem. **23**, 387 (1983).
[7] E. Gratton and M. Limkeman, Biophys. J. **44**, 315 (1983).
[8] J. Baumann, Ph.D. Thesis, Institute for Inorganic and Physical Chemistry, University of Berne, Berne, 1984.
[9] J. R. Lakowicz and B. P. Maliwal, Biophys. Chem. **21**, 61 (1985).
[10] T. Hugentobler, Ph.D. Thesis, Institute for Inorganic and Physical Chemistry, University of Berne, Berne, 1987.
[11] I. S. S., Inc., 2401 S. Neil Street, Champaign, IL 61820, model GREG 200: Technical Data.
[12] J. R. Lakowicz, G. Lazko, and I. Gryczynski, Rev. Sci. Instrum. **57**, 2499 (1986).
[13] J. R. Lakowicz, M. L. Johnson, I. Gryczynski, N. Joshi, and G. Lazko, J. Phys. Chem. **91**, 3277 (1987).
[14] S. Kinoshita and T. Kushida, Rev. Sci. Instrum. **53**, 469 (1982).
[15] W. R. Ware, M. Pratinidhi, and R. K. Bauer, Rev. Sci. Instrum. **54**, 1148 (1983).
[16] S. Canonica, J. Forrer, and U. P. Wild, Rev. Sci. Instrum. **56**, 1754 (1985).
[17] M. Köchel, K. Hirsch, and H. Salzmann, Rev. Sci. Instrum. **58**, 136 (1987).
[18] Products for Research, Inc., 78 Holton Street, Danvers, MA 01923, Catalog 104, 1983.
[19] Hamamatsu Photonics K.K., Hamamatsu City, 430 Japan, Photomultiplier Tubes Catalog, 1986.
[20] S. Bergamasco, G. Calzaferri, and K. Hädener (in preparation).